

# Production of dimethyl carbonate by gas-phase oxidative carbonylation of methanol over Cu/Y zeolite: Mechanism and kinetics

Mauro Álvarez, Pablo Marín, Salvador Ordóñez\*

Catalysis, Reactors and Control Research Group (CRC), Dep. of Chemical and Environmental Engineering, University of Oviedo, Julián Clavería 8, 33006 Oviedo, Spain

## ARTICLE INFO

### Keywords:

Fuel additive  
Green chemistry  
Zeolite catalyst  
Kinetic model  
Organic carbonate

## ABSTRACT

Dimethyl carbonate (DMC) has become into an appealing fuel additive for reducing the formation of pollutants during combustion and, together with the post-combustion treatment, allowing to fulfill the most stringent environmental regulations. Although the production of this chemical is still an open issue, the oxidative carbonylation of methanol catalyzed by solids and with reactants and products in the gas phase has been proposed to replace the homogeneous commercial process (CuCl in aqueous phase). In this work, we propose the use of a Cu/Y zeolite (prepared by solid-state ion exchange with copper (I) chloride) as alternative catalyst for this purpose, optimizing the reaction conditions and proposing a rigorous kinetic model for this reaction. For accomplishing this aim, gas phase reaction was performed in a continuous fixed-bed reactor. Temperature (100–200 °C) played a critical role in product distribution, DMC being the main product at 120 °C. The influence of different reactant (CH<sub>3</sub>OH/CO/O<sub>2</sub>) concentrations on reaction rate and product distribution was determined at 120 °C. The experimental data have been successfully fitted to a kinetic model, derived from the mechanism of the reaction.

## 1. Introduction

Dimethyl carbonate (DMC) has gaining increasing interest as fuel additive in the last decades, although its first identified applications were as solvent and methylating agent [1–4]. As benign methylating agent, DMC can replace other toxic compounds, such as, dimethyl sulfate or methyl halides. An application of importance is the use in carbonylation reactions, replacing highly toxic phosgene, and the production of diphenyl carbonate by transesterification with phenol. This compound in an intermediate in the production of polycarbonates polymers [5–9]. The applications as solvent have raised in the last years, due to the exemption of the definition of volatile organic compound (VOC) by the US Environmental Protection Agency [10]. Thus, DMC has replaced other popular solvents, such as, methyl ethyl ketone and it has increased the use as electrolyte in lithium-ion batteries.

The use of DMC as fuel additive has also gained attraction in the last decades. The high oxygen content of DMC and its good blending octane makes it an excellent fuel additive, reducing the emissions of internal combustion engines [11–13]. Compared to other oxygenated additives, DMC presents a better efficiency in reducing the emissions of NO<sub>x</sub>, CO, and soot with the only disadvantage of a lower heating value [14–17].

The environmental regulations are becoming stricter and, in some cases, post-combustion treatment alone would not be enough (or very expensive) to meet the standards. These excellent properties, together with its non-toxicity and the exemption from the definition of VOC, convert DMC into a great alternative to other fuel additives, e.g., alkylcarbonates and even methyl tert-butyl ether (MTBE).

DMC is synthesized from methanol according to different routes and raw materials. Nowadays, the main ultimate raw material is natural gas, but biogas, biomass or even green hydrogen can be easily incorporated to the production process. This is quite interesting from the point of view of global warming. The use of green DMC as, for example, fuel additive would also be part of the biofuel percentage required regular fuels.

The direct synthesis from methanol and carbon dioxide is highly desirable to incorporate as raw material residual carbon dioxide from other processes. These processes are critical for the implementation of a circular economy, reducing the consumption of raw materials and the emissions of greenhouse gases. However, this reaction is highly limited by the equilibrium, leading to extremely low yields [18]. To overcome these drawbacks different strategies have been proposed in the literature, but more research is required to obtain a scalable process [19].

The traditional production process of DMC is based on the reaction of

\* Corresponding author.

E-mail address: [sordonez@uniovi.es](mailto:sordonez@uniovi.es) (S. Ordóñez).

<https://doi.org/10.1016/j.fuproc.2023.107805>

Received 16 March 2023; Received in revised form 14 April 2023; Accepted 22 April 2023

Available online 28 April 2023

0378-3820/© 2023 The Authors. Published by Elsevier B.V. This is an open access article under the CC BY-NC-ND license (<http://creativecommons.org/licenses/by-nc-nd/4.0/>).

methanol and phosgene. Given the high toxicity of phosgene, this process has been replaced by other ones more environmentally friendly [18,20,21]. One of these processes, which has achieved successful industrialization by Enichem in the 80s, is the oxidative carbonylation of methanol. This process is based on the reaction between liquid methanol and a gas made of a mixture of CO and O<sub>2</sub> in the presence of cuprous chloride, acting as homogeneous catalyst. Given the low solubility of the catalyst, the reactor operates with a slurry of the copper salt [8,19]. This process has some drawbacks, such as, the use of a three-phase reactor with partial vaporization of the reaction media because of the exothermic reaction, which can be dangerous and difficult to operate, the loss of catalyst, equipment corrosion and complex product separation. For this reason, different alternatives to produce DMC are being investigated [1,2].

UBE developed another DMC synthesis route based on a two-step reaction process. In a first reactor, methanol is transformed into methylnitrite by reaction with nitrogen monoxide. Then, in a second reactor, this intermediate compound reacts with CO over a palladium-copper chloride catalyst to produce DMC [19]. However, this process requires two reactors and uses toxic reactants and intermediates.

There is a lot of interest in developing an oxidative carbonylation process able of operating with all the reactants in the gas phase and using solid catalysts [22]. Some authors have successfully studied as catalysts copper chlorides supported on activated carbon or silica [23,24]. The active carbon-based catalysts presented good selectivity towards DMC for methanol, but not for CO, which was easily oxidated to CO<sub>2</sub> and formed undesired byproducts (chloromethane) [25,26].

Due to these problems, research efforts moved towards the use of Cu-exchanged zeolites as catalysts [27]. Several types of zeolite supports have been evaluated by different authors, such as, X zeolite [28,29], Y zeolite [22,30–32], mordenite [32] and ZSM-5 [27,29,32]. Also Al-KIT-6 [33] and MCM-41 [34] have been proposed as supports. Previous studies had showed that the Y zeolite support was better in terms of activity and selectivity to DMC than other zeolites, like ZSM-5, mordenite and X zeolites [32].

Oxidative carbonylation of methanol has successfully been studied by spectroscopic techniques. The identified reaction intermediates have been found useful to postulate a mechanism for the reaction. First, methanol is adsorbed on surface bound-Cu<sup>+</sup> active centers to form a methoxide species, Cu-OCH<sub>3</sub>. Then, gas-phase CO is inserted on the adsorbed methoxide species and, finally, DMC is formed by dehydration with another methanol molecule [30,35–37]. The strength of CO and methoxide adsorption affects the reaction. A strong adsorption of CO actually blocks the sites for methoxide formation, but does not participate in DMC formation [29]. The better performance of Cu/Y zeolites for the oxidative carbonylation reaction is associated to an easier adsorption of methanol, due to a weaker adsorption of CO in comparison to the other Cu-exchanged zeolites [36]. The balanced acidity of the Y zeolite support, with a Si/Al ratio of 6, is also useful to catalyze the dehydration steps of the reaction mechanism.

The Y zeolite support, with a Si/Al ratio of 6, offers balanced acid and hydrophilic properties, as required by the dehydration steps of the reaction mechanism, which catalyze the formation of DMC. However, too strong acidity can also trigger other undesired dehydration reactions, resulting in the formation of dimethoxymethane (DMM), dimethyl ether (DME) and methyl formate (MF) by-products [27,28].

Despite the Cu/Y zeolite exhibits the best performance, there are not kinetic models available for this catalyst. The present work wants to fill this gap and, for the first time ever, a mechanistic kinetic model is presented for Cu/Y zeolites. This model constitutes the first step needed to accomplish the scale-up of a production process of DMC based on oxidative carbonylation of methanol in the gas phase.

To achieve this objective, first, the Cu/Y zeolite has been prepared via solid-state ion exchange. Then, reaction experiments have been carried out in a continuous fixed-bed reactor to evaluate the stability of the catalyst and determine the influence of the main operating variables

(temperature and reactant concentration). Finally, a kinetic model has been developed based on the reaction mechanism, and this model has been fitted to the experimental data.

## 2. Materials and methods

### 2.1. Chemical reagents

Solid and liquid reagents used in this study are: copper (I) chloride (97%, Alfa Aesar), methyl formate (Sigma Aldrich, reagent grade 97%), dimethoxymethane (Sigma Aldrich, reagent plus >99%), dimethyl carbonate (Sigma Aldrich, anhydrous >99%) and methanol (VWR, AnalaR NORMAPUR >99.8%). All the gases used as reactants and for the analysis by gas chromatography were provided by Air Liquide: N<sub>2</sub> (Alphagaz 1), O<sub>2</sub> (Alphagaz 1), He (Alphagaz 1), air (Alphagaz 1), CO (>99%) and dimethyl ether (>99.9%). The catalyst support was the ammonium Y zeolite with a Si/Al ratio of 6, supplied by Zeolyst International.

### 2.2. Catalyst preparation

The catalyst has been prepared according to a solid-state ion exchange (SSIE) procedure. First, the zeolite powder and copper (I) chloride solids were mixed in a mass ratio of 4:1. Then, the mixture was loaded into a stainless steel tube and heated in He stream to 650 °C for 20 h to promote the volatilization of the copper salt and ion exchange into the zeolite [28,30,32]. Finally, the catalyst was pelletized and sieved to a particle size in the range 0.355–0.100 mm.

### 2.3. Catalyst characterization

The copper content of the Cu/Y zeolite was determined by dissolving the samples in aqua regia and the analysis of the solution using an inductively coupled plasma mass spectrometer (ICP-MS).

The catalyst morphological properties were obtained using different techniques. Surface area and internal porosity were measured on a Micromeritics ASAP 2020 Plus. Diffractograms of the catalysts were obtained via X-ray powder diffraction (XRD) on a Bruker D8 Discover diffractometer with a radiation scanning 2 $\theta$  range between 5 and 90°.

### 2.4. Experimental device

The oxidative carbonylation reaction tests were carried out in a stainless-steel fixed-bed tubular reactor operated continuously. The reactor (6.8 mm of internal diameter) was loaded with 2 g of catalyst (catalytic bed length of 72 mm) and upstream the catalytic bed the reactor tube was filled with glass spheres (1 mm). Ideal plug flow regime in the catalytic bed was ensured using a ratio of reactor diameter to solid particle size higher than 10 (11) and a ratio of reactor length to solid particle size higher than 50 (108) [38]. Temperature inside the reactor was measured using a thermocouple placed below and close to the catalytic bed. The measurements of this thermocouple were used by a PID feedback controller to regulate the power of the electrical oven that surrounded the reactor tube. The oven is also equipped with 4 thermocouples that measure the temperature along the reactor outside the tube to evaluate if the operating conditions were isothermal. These conditions were achieved by diluting the catalyst with glass, as explained above, and by operating the reactor at low conversion (below 10% for the tests aimed at measuring the reaction rate and used in the kinetic analysis).

Gas flowrates were set using mass flow controllers provided by Bronkhorst, while the liquids were introduced using a syringe pump. The WHSV was typically 4.65 Nm<sup>3</sup>/h kg<sub>cat</sub>. All the experiments were performed at atmospheric pressure. Most of the tubing of the equipment was covered by heating tape, set to 120 °C to prevent condensation of any compounds.

The effluent of the reactor was analyzed on-line using a gas chromatograph (Agilent HP-6890 N), equipped with a thermal conductivity detector (TCD) and a flame ionization detector (FID) placed in series. Reactants and products were separated using two columns: a HP Plot Q (to separate CO<sub>2</sub> and the oxygenated organic compounds) and a HP MoleSieve 5A (to separate CO, O<sub>2</sub> and N<sub>2</sub>). The latter column was laid out on-line or off-line using a multi-port valve.

### 2.5. Reaction tests

The reaction tests were carried out in the continuous fixed-bed reactor by feeding a mixture of the reactants (methanol, CO and O<sub>2</sub>) and N<sub>2</sub> acting as balance gas.

The kinetics of the reaction was studied at 120 °C and WHSV of 4.65 Nm<sup>3</sup>/h kg<sub>cat</sub>. Reactants concentrations were changed, and the corresponding reaction rates of product formation determined using the outlet concentrations measured in steady state. The operating conditions were selected to maintain conversion below 10%. By this way, the fixed-bed is operated in the differential reactor regime, i.e., temperature, concentration and reaction rate being approximately the same for all the catalyst particles of the reactor. According to this, the following expression were used to estimate the reaction rates:

$$r_i = \frac{dF_i}{dW} \approx \frac{F_i - F_{i0}}{W} = \frac{F_0}{W} (y_i - y_{i0}) \quad (1)$$

Where  $r_i$  is the reaction rate of compound  $i$ ,  $F_i$  is the molar flow rate,  $y_i$  is the molar fraction,  $W$  is the mass of catalyst and  $F_0/W$  is the space velocity (WHSV).

## 3. Results and discussion

### 3.1. Catalyst characterization

The solid-state ion exchange procedure used for the preparation of the catalyst led to zeolites with a copper content of 5.7 wt%. This value is slightly lower than the one reported by other authors using the same preparation method [30]. Fresh and aged catalyst samples showed the same copper content.

The results of nitrogen adsorption tests are shown in Table 1. The Cu-exchanged zeolites exhibit lower BET surface area than the bare Y zeolite, which may be caused by the blockage or collapse of some micropores during the copper exchange, as suggested by the observed decreases of microporous volume. Mesoporous volume remains practically constant, which means that this type of channels are quite stable. The results obtained for the used Cu/Y zeolite (time on stream 100 h at 120 °C) are very close to that of the fresh one, except for a slight decrease in the microporous volume. These results confirm that the Cu/Y zeolite presents a good structural stability at reaction conditions.

Fig. 1 presents the XRD patterns of the NH<sub>4</sub>-Y zeolite and the Cu/Y zeolite, prepared by solid-state ion exchange (SSIE). The most relevant peaks of the Y zeolite are located at Bragg's angle of 6, 10, 12, 16, 19, 20 and 24, being the first one the peak with the highest intensity. No new peaks are detected after SSIE but the intensity of the characteristic peak of zeolite Y (6.13°) decreased for the exchanged zeolite, showing a crystallinity decrease of 26%.

**Table 1**  
Surface area and pore volume of Y zeolite and fresh and used Cu/Y zeolite.

Sample	BET surface (m <sup>2</sup> /g)	Mesoporous volume (cm <sup>3</sup> /g)	Microporous volume (cm <sup>3</sup> /g)
NH <sub>4</sub> -Y zeolite	693	0.155	0.262
Cu/Y zeolite, fresh	575	0.149	0.219
Cu/Y zeolite, used	563	0.151	0.200

### 3.2. Determination of the reaction scheme

The analysis of the reactor effluent revealed the presence of three products: dimethyl carbonate (DMC), dimethoxy methane (DMM) and dimethyl ether (DME). The product distribution is highly affected by temperature, as depicted in Fig. 2. This test was carried out at WHSV of 4.65 Nm<sup>3</sup>/h kg<sub>cat</sub> with a feed concentration (in mole %) of: 16% methanol, 42% CO and 8% O<sub>2</sub>.

At low temperature, the selectivity of DMC and DMM are high, respectively, 60% and 40% at 100 °C. However, on increasing temperature the selectivity of DMC decreases considerably, falling to zero at 200 °C. DMM selectivity increases from 40% at 100 °C to a maximum of 61% at 150 °C and, then, decreases towards zero. The decrease of DMC and DMM selectivity is associated to an increase in DME formation with a selectivity increasing sharply with temperature (at 200 °C DME is the main product with a selectivity of 87%).

According to these experimental results, the reaction scheme of Fig. 3 has been proposed. Methanol can react according to three parallel reactions: oxidative carbonylation to DMC, oxidation and aldol condensation to DMM, and dehydration to DME. The stoichiometry of these reactions is different; both DMC and DMM formation require oxygen, but only DMC synthesis consumes CO. As shown in Fig. 2, the rates of these reactions are highly dependent on temperature. This is explained by the functional properties of the Cu/Y zeolite catalyst, offering different types of reaction sites: Cu sites for the oxidation reactions and acid sites of the zeolite for dehydration reactions. The Cu sites are activated at a lower temperature and, consequently, DMC and DMM are the main products in the range 100 to 150 °C.

The catalytic activity of the acid sites of the Y zeolite has been tested by means of reaction tests with a feed made of 16% methanol in nitrogen (WHSV = 4.65 Nm<sup>3</sup>/h kg<sub>cat</sub>).

At 120 °C, there were no conversion. At 150 °C, methanol conversion was 0.34%, being DME the only product. The test was repeated using the un-exchanged Y zeolite and methanol conversion was 0.8% at the same conditions. This result demonstrates that methanol dehydration to DME is catalyzed by acid sites of the Y zeolite.

Given that DMC and DME selectivity are inversely correlated, it is plausible to consider that part of the formed DME can be produced by decomposition of DMC. To test this hypothesis a set experiments has been done using DMC as reactant. The space velocity was the same as in the previous tests (4.65 Nm<sup>3</sup>/h kg<sub>cat</sub>). At 120 °C and a feed gas of 1.5% DMC, the reaction products were DME and CO<sub>2</sub> with a conversion of 28.7% for the Cu/Y zeolite catalyst. The test was repeated at the same conditions for the un-exchanged Y zeolite, resulting in a conversion of 100%. This suggests DMC can easily decompose to DME on the acid sites of the Y zeolite. Additional tests were carried out at different DMC feed concentrations and reaction temperatures, as summarized in Table 2.

An increase in DMC feed concentration led to a decrease in conversion, which can be attributed to the strong adsorption of DMC on the catalyst acid sites. Conversely, an increase in temperature resulted in an increase in conversion, thereby explaining the rise in DME selectivity seen in Fig. 2.

Considering these findings, the optimum reaction temperature to maximize DMC yield is 120 °C. At this temperature, DMC and DMM are the only reaction products, DMC decomposition to DME being negligible. Hence, the following reaction experiments will be carried out at 120 °C. It should be noted that DMM co-product can also be interesting with several industrial applications, such as, solvent, fuel additive or feedstock for the manufacture of many chemicals. The separation of these products might be done by distillation, since their boiling points differ in >20 °C.

### 3.3. Stability of the catalyst

The stability of the catalyst upon time has been evaluated by operating the reactor, loaded with fresh catalyst (2 g), at 120 °C and with a

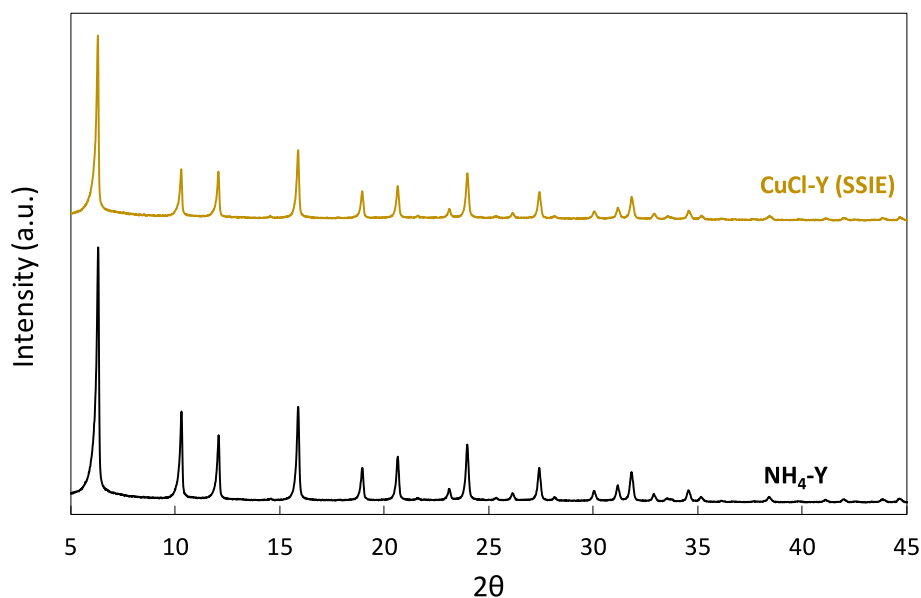


Fig. 1. Comparison between XRD patterns of commercial and exchanged Y zeolite.

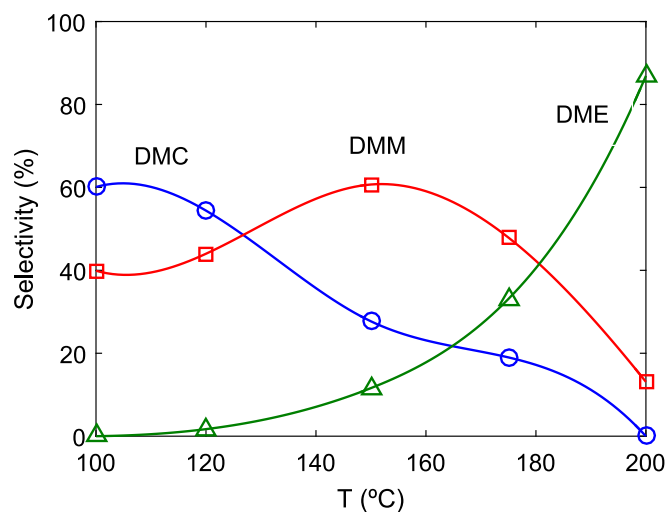


Fig. 2. Influence of temperature on product selectivity:  $\circ$  DMC,  $\square$  DMM and  $\triangle$  DME. Reaction conditions: WHSV =  $4.65 \text{ Nm}^3/\text{h kg}_{\text{cat}}$ , 16% methanol, 42% CO and 8%  $\text{O}_2$  (mole fraction).

gas feed of 16% methanol, 42% CO and 8%  $\text{O}_2$ . The space velocity WHSV was set to  $4.65 \text{ Nm}^3/\text{h kg}_{\text{cat}}$ . These conditions were maintained constant for 100 h, the reactor effluent being analyzed on-line. Fig. 4a depicts the evolution of DMC formation rate.

In the first 1–2 h time on stream, DMC product was not observed in the reactor effluent. This could be attributed to the adsorption of DMC or some reactant or reaction intermediate on the catalyst surface. Note that the acid character of the Y zeolite support makes it a good material for the adsorption of oxygenated compound like DMC, as explained in section 3.2. Once the surface of the catalyst is saturated, DMC appeared in the reactor effluent.

After this initial period, DMC formation rate decreased a bit until ca. 10 h and, then, it remained practically constant for the rest of the test. This behavior indicates that the catalyst did not suffer from deactivation for, at least, 100 h of operation and that only a short initial stabilization period is observed.

Water is generated as a product in DMC synthesis, and it is well-known that water can adsorb on zeolites [28]. In order to elucidate if

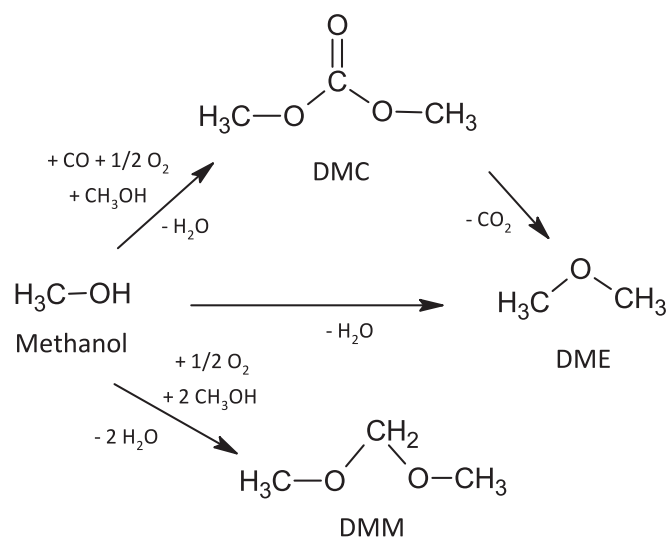


Fig. 3. Reaction scheme of methanol oxidative carbonylation and aldol condensation.

Table 2

DMC decomposition on Cu/Y zeolite. Conditions: WHSV =  $4.65 \text{ Nm}^3/\text{h kg}_{\text{cat}}$ .

T (°C)	% mol DMC	Conversion (%)
120	1.5	28.7
120	3.8	23.9
120	6.6	16.7
150	6.6	45.2
200	6.6	98.5

water has some influence on the stability of the catalyst, an experiment in which additional water was introduced in the reactor feed had been carried out, as shown in Fig. 4b. This test was conducted in the same way as the previous stability test until  $t = 40$  h. At this time, the concentration of water in the reactor feed was stepped to 4% mol. This produced a fall of DMC formation rate to zero, which is explained by the adsorption of water on the zeolite with blockage of the reaction sites needed for the reaction. At  $t = 50$  h, water was removed from the feed.

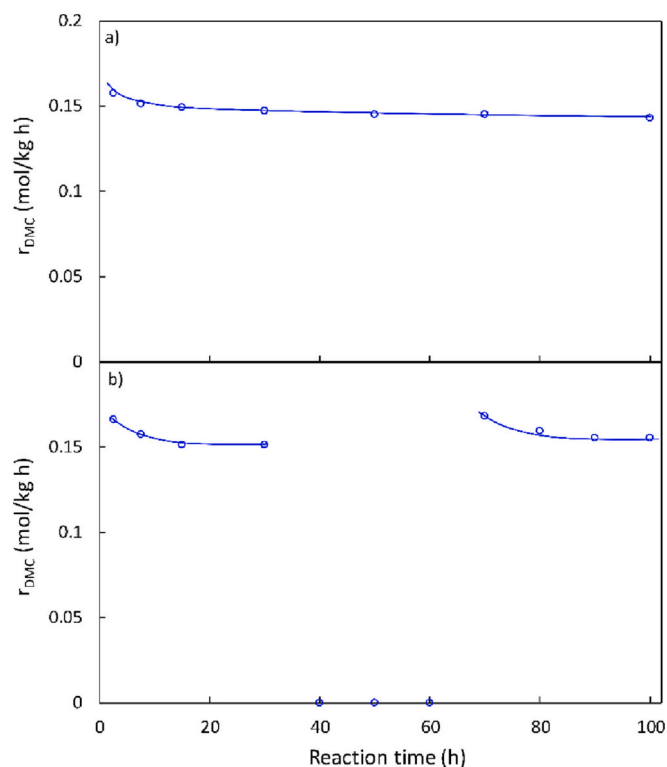


Fig. 4. a) Stability test. b) Study of the influence of water (4% water between 40 h and 50 h, heating between 50 h and 60 h). Reaction conditions: 120 °C, WHSV = 4.65 Nm<sup>3</sup>/h kg<sub>cat</sub>, 16% methanol, 42% CO and 8% O<sub>2</sub> (mole fraction).

However, DMC formation was not fully recovered. Then, temperature was raised to 320 °C for a few hours in the presence of a N<sub>2</sub> stream to facilitate water desorption. After this treatment, temperature was set again to 120 °C and the reaction feed was introduced ( $t > 60$  h). As shown in Fig. 4b, the formation rate of DMC exhibited a similar behavior to that obtained with fresh catalyst at the beginning of the catalyst: in the first 1–2 h, no product is formed and, then, it is reported a slight decrease in reaction rate for ca. 10 h.

According to these results, it can be concluded that the loss of activity caused by water is reversible and can be completely recovered by regeneration at higher temperature. The adsorption of the water generated as reaction product can explain the decrease of reaction rate observed at the beginning of the test (and after regeneration). Initially the catalyst surface is free of adsorbed water and the water generated as product may remain adsorbed on the catalyst, decreasing the available active sites for the reaction. However, after a few hours, the equilibrium between the adsorbed water and the gas-phase water is established, which is traduced into the observed constant formation rate of DMC.

### 3.4. Influence of the reactants concentration

The aim of this section is to study the influence of methanol, carbon monoxide and oxygen reactants on the reaction rate. The tests were carried out at a temperature of 120 °C, total pressure of 100 kPa, and space time WHSV of 4.65 Nm<sup>3</sup>/h kg<sub>cat</sub> (total flow gas rate of 155 NmL/min). A temperature of 120 °C has been selected, because as discussed in section 3.2, this value avoids the formation of DME as by-product (Fig. 2); the only reaction products being DMC and DMM.

The space time has been selected to maintain the conversion of the reactor below 10% in all the tests. This way, the concentration of the reaction products is kept low, reducing the influence on the observed reaction rates of other undesired reactions, such as, the decomposition of DMC or the adsorption of the water product on the catalyst. In addition, the fixed-bed reactor can be modeled as a differential reactor,

e.g., concentrations and reaction rates approximately the same for all the catalyst particles. The reaction rates of formation of DMC and DMM have been calculated using the concentrations of these compounds in the reactor effluent (see section 2.5 for more details).

The composition of the reactants has been varied in the following ranges (in mole percentage): 6–16% for O<sub>2</sub>, 7–27% for methanol and 18–80% for CO (the flow rate of N<sub>2</sub> was adjusted to maintain the same total gas flow rate and WHSV in all the tests).

The results of the experiments are depicted as symbols in Fig. 5. It can be observed that DMC and DMM reaction rates increase on increasing methanol partial pressure, with DMC reaction rate having a higher dependence on the concentration of this reactant (Fig. 5a). The dependence is not linear, since reaction rates of both products are levelled for high methanol concentrations. This behavior is consistent with an inhibition caused by the adsorption of methanol at high concentration.

A similar behavior is observed for oxygen with reaction rate increasing when oxygen concentration is raised (Fig. 5b). This reactant is involved in both reactions, DMC and DMM formation. As suggested by different authors, oxygen is responsible of the re-oxidation of the active centers of the catalyst [36].

Regarding the effect of CO partial pressure, it is observed a high dependence on DMC formation rate (Fig. 5c). This suggests that CO might be involved in the rate-limiting steps of the reaction mechanism. For the case of DMM formation, a slight decrease on reaction rate was observed on increasing CO concentration. Given that CO is not a reactant in DMM formation, this little decrease points to an inhibitory effect caused by CO adsorption. Thus, it is well-known that CO adsorbs on Cu (I) [30] and, hence, it may compete with methanol for the reaction active sites. At high CO concentration, this effect is more marked, explaining the observed decrease in DMM reaction rate.

Before fitting the experimental data to a kinetic model, it has been evaluated if these data are affected by diffusional limitations. If it were the case, the observed reaction rates would be lower than the intrinsic ones and it would be more complex to fit kinetic equation based on the reaction mechanism. In the literature, different criterion and dimensionless factors have been proposed to discard the influence of diffusional effect on reaction rate data [39]. Here, the Wagner module has been used for intraparticle diffusion:

$$M_W = \frac{L^2}{D_{Ae}} \left( \frac{-r_A}{C_A} \right)_{obs} < 0.15 \quad (2)$$

Where  $L = 3.8 \cdot 10^{-5}$  m is the characteristic catalyst dimension ( $d_p/6$  for spherical particles),  $C_A$  and  $-r_A$  are, respectively, the molar concentration and observed reaction rate of the limiting reactant, and  $D_{Ae}$  is the effective diffusion coefficient,  $D_{Ae} = D_{K,A}(\epsilon_{int}/\tau_p) = 5.9 \cdot 10^{-8}$  m<sup>2</sup>/s. Knudsen diffusion ( $D_{K,A}$ ) has been assumed as the most important diffusion mechanism in the Cu/Y zeolite, given the size of the catalyst pores (0.8 nm) [40]. The Wagner module is  $M_W = 8 \cdot 10^{-4}$  for the highest reaction rate (0.29 mol/kg<sub>cat</sub> h). This means that pore diffusion resistance can be neglected ( $M_W < 0.15$ ).

The Carberry number is commonly used to estimate extraparticle mass transfer [39]:

$$Ca = \frac{1}{ak_f} \left( \frac{-r_A}{C_A} \right)_{obs} < 0.05 \quad (3)$$

In this expression  $a$  is the specific external surface of the catalyst particle ( $a = 6/d_p$  for spheres),  $k_f = Sh D_A/d_p$  is the film mass transfer coefficient,  $D_A$  is the molecular diffusion coefficient of methanol ( $7.1 \cdot 10^{-6}$  m<sup>2</sup>/s) and  $Sh \approx 2$  is the Sherwood number. The estimated value of Carberry number at the highest reaction rate was  $Ca = 1.4 \cdot 10^{-5}$ , considerably lower than the limit of 0.05. Hence, extraparticle mass transfer resistance is also negligible.

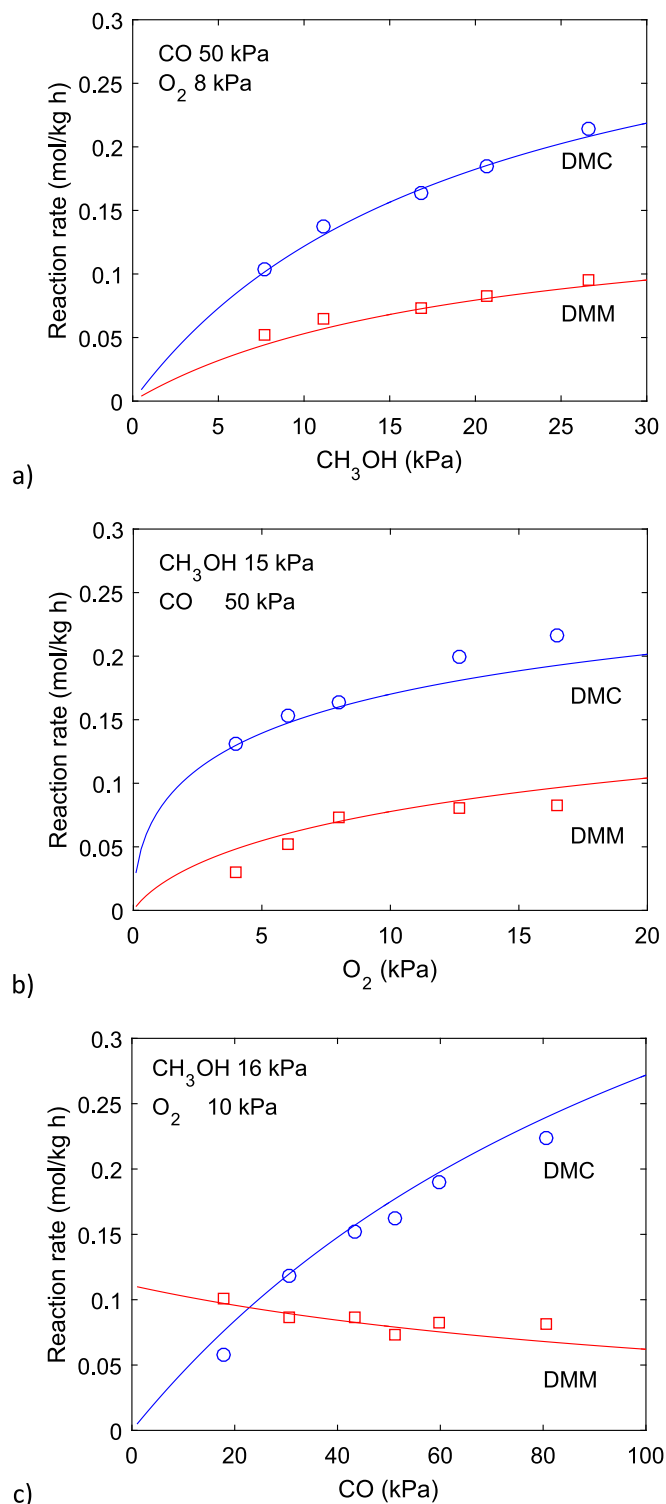


**Fig. 5.** Effect of methanol (a), oxygen (b) and carbon monoxide (c) partial pressures on the reaction rates of DMC (○ blue) and DMM (□ red) at 120 °C. Symbols: experiments. Lines: model predictions. (For interpretation of the references to colour in this figure legend, the reader is referred to the web version of this article.)

### 3.5. Reaction mechanism and kinetic model

The reaction mechanism for the synthesis dimethyl carbonate by the gas-phase oxidative carbonylation over Cu–Y zeolites has already been investigated by different authors [28,30,35,36,41]. The steps of the

reaction mechanism are summarized in Fig. 6. First, methanol adsorbs molecularly on Cu<sup>+</sup> cations (1) [35]. Then, adsorbed methanol reacts to form mono-methoxide (MM) species (2). This step has been observed in the presence of gas-phase O<sub>2</sub>, but also in its absence, at least to some extent. This suggests a participation of lattice oxygen of CuO<sub>x</sub> aggregates and points to a Mars-van-Krevelen mechanism [36,42].

The adsorption of a second molecule of methanol results in the formation of di-methoxide (DM) species (3). Zhang et al. [32,35] proposed two parallel paths for the formation of DMC: (a) the insertion of CO on mono-methoxide species to generate a monomethyl carbonate (MMC) intermediate (4), able of reacting with another methanol molecule to form DMC (5), and (b) the insertion of CO on di-methoxide species to form directly the DMC product (6). Conversely, Engeldinger et al. [36,41] proposed that monomethyl carbonate (MMC) intermediate is formed by the simultaneous adsorption of methanol and CO on the same Cu site.

There is an agreement in the literature in considering the insertion of CO as the slow or rate-limiting step of the mechanism (steps 4 and 6 of Fig. 6) [30,35]. Hence, a kinetic model for the formation of DMC has been developed. The formation rate of DMC is obtained as the sum of the rate-limiting elementary steps of the two parallel routes of the mechanism, eq. (4):

$$r_{DMC} = r_4 + r_6 = k_4 p_{CO} \theta_{MM} + k_6 p_{CO} \theta_{DM} \quad (4)$$

The fraction of adsorbed methanol ( $\theta_M$ ), mono-methoxide ( $\theta_{MM}$ ) and di-methoxide ( $\theta_{DM}$ ) species are obtained assuming the steps before the rate-limiting steps are fast enough to be at equilibrium. The regeneration of oxygen in the CuO<sub>x</sub> aggregates by gas-phase O<sub>2</sub> is also considered in equilibrium. Using these considerations, the following expressions are obtained:

$$CuO_{x-1} + \frac{1}{2} O_2 \rightleftharpoons CuO_x, \quad \frac{\theta_{CuO_x}}{\theta_{CuO_{x-1}}} = K_{O_2} p_{O_2}^{1/2} \quad (5)$$

$$\theta_M = K_1 p_M \theta \quad (6)$$

$$\theta_{MM} = K_2 \theta_M \frac{\theta_{CuO_x}}{\theta_{CuO_{x-1}}} = K_1 K_2 K_{O_2} p_M p_{O_2}^{1/2} \theta \quad (7)$$

$$\theta_{DM} = K_3 \frac{\theta_{MM} p_M}{p_{H_2O}} = K_1 K_2 K_3 K_{O_2} \frac{p_M^2 p_{O_2}^{1/2} \theta}{p_{H_2O}} \quad (8)$$

The fraction of empty Cu sites ( $\theta$ ) are determined from a balance to the total sites, Eq. (9). In this balance, fractions of adsorbed MMC and DMC have been considered negligible compared to other species for two reasons. First, the spectroscopy transient experiments reported in the literature identified an increase in the adsorbed species at the same time as DMC increased in the gas phase, which can be attributed to an easy desorption of DMC [36]. Second, the experiments of the present work were done at low conversion, in the differential reactor regime. At these conditions, the concentration of DMC in the gas phase is low, favoring desorption and reducing the adsorbed fraction of DMC and MMC.

The adsorption of CO on Cu sites is very important; however, the formation of methoxide species in these sites has been found to inhibit CO adsorption significantly, as reported experimentally [35,36] and using the density functional theory [43]. The corresponding term for CO adsorption ( $\theta_{CO}$ ) has been included in the balance to the total sites, but its significance as part of the kinetic model will be evaluated later when fitting to the experimental data.

$$1 = \theta + \theta_M + \theta_{MM} + \theta_{DM} + \theta_{CO} \quad (9)$$

$$\theta_{CO} = K_{CO} p_{CO} \theta \quad (10)$$

Solving Eqs. (5) to (10) for  $\theta$  and substituting on eq. (4), the following kinetic expression is obtained for DMC formation.

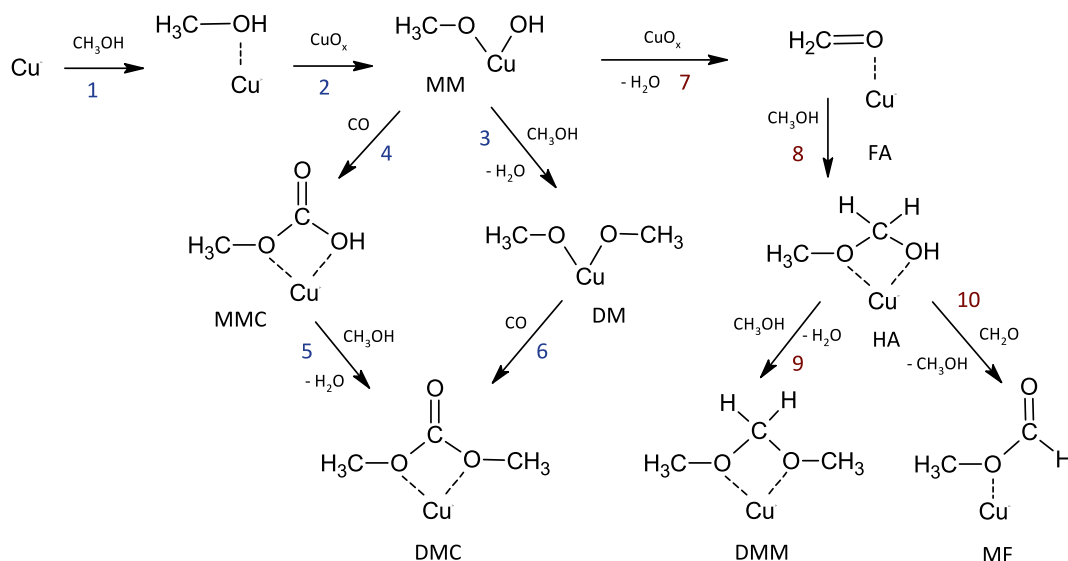


Fig. 6. Mechanism of dimethyl carbonate synthesis on Cu/Y-zeolite (MM: mono-methoxide; DM: di-methoxide; MMC: monomethyl carbonate; DMC: dimethyl carbonate; FA: formaldehyde; HA: hemiacetal; DMM: dimethoxy methane; MF: methyl formate).

$$r_{DMC} = \frac{k_4 K_1 K_2 K_{O_2} P_M P_{O_2}^{1/2} P_{CO} + k_6 K_1 K_2 K_3 K_{O_2} \frac{P_M^2 P_{O_2}^{1/2} P_{CO}}{P_{H_2O}}}{1 + K_1 P_M + K_1 K_2 K_{O_2} P_M P_{O_2}^{1/2} + K_1 K_2 K_3 K_{O_2} \frac{P_M^2 P_{O_2}^{1/2}}{P_{H_2O}} + K_{CO} P_{CO}} \quad (11)$$

The oxidative carboxylation of methanol on Cu/Y zeolites generates DMC as main product, but also other by-products are formed like dimethoxy methane (DMM) and methyl formate (MF). These products are the consequence of a further oxidation of adsorbed methoxide species (MM) via formaldehyde (FA) intermediate, as shown in the mechanism of Fig. 6. This oxidation takes place with participation of lattice oxygen of  $CuO_x$  aggregates, like the formation of methoxide species, according to a Mars-van-Krevelen mechanism (7). Formaldehyde intermediate is very reactive, and it can generate a hemiacetal (HA) intermediate by reaction with methanol (8). Then, the hemiacetal intermediate can react with a second methanol molecule according to an aldol condensation reaction to generate DMM (9) or, otherwise, it can be oxidized with formaldehyde (10) to methyl formate (MF) [35,42]. It is well known that the reaction of formaldehyde and methanol to DMM can be catalyzed by acid sites of the zeolite [44].

As discussed in Section 3.2, the reaction products observed in the present work at low temperature (120 °C) were only DMC and DMM. Hence, the formation of methyl formate (MF, step 10) is discarded for the development of the kinetic model. Given the high reactivity of formaldehyde, which was not detected as product (neither in other works from the literature), it is plausible to consider the formation of formaldehyde (step 7) as the rate-limiting step of this reaction path. This step involves the reaction of adsorbed mono-methoxide specie with lattice oxygen of  $CuO_x$  aggregates, eq. (12). The fraction of available  $CuO_x$  sites is determined from a site balance considering the regeneration of  $CuO_{x-1}$  sites with gas-phase  $O_2$  is in equilibrium, eq. (13):

$$r_{DMM} = r_7 = k_7 \theta_{MM} \theta_{CuO_x} \quad (12)$$

$$\theta_{CuO_x} = \frac{K_{O_2} P_{O_2}^{1/2}}{1 + K_{O_2} P_{O_2}^{1/2}} \quad (13)$$

The combination of Eqs. (7), (12) and (13) produces the following kinetic expression for the rate of DMM formation:

$$r_{DMM} = \frac{k_7 K_1 K_2 K_{O_2}^2 P_M P_{O_2}}{(1 + K_{O_2} P_{O_2}^{1/2}) DEN} \quad (14)$$

Where DEN is the denominator of Eq. (11). Since reaction steps 8 and 9 are fast (compared to the rate-limiting step) and the gas-phase concentration of DMM is low (the kinetic tests were carried out at low conversion), it has been assumed that the fraction of adsorbed HA and DMM is low in comparison with the other species. Hence, the same expression for the empty Cu sites ( $\theta = 1/DEN$ ) as in DMC formation rate expression is obtained, Eq. (11).

### 3.6. Fitting of the kinetic model

In this section, the kinetic model developed from the reaction mechanism has been fitted to the experimental data reported in Section 3.4. Both DMC and DMM formation rates have been fitted together, since both reactions are intrinsically related, and their kinetic equations share some adsorption constants. The fitting has been done with the help of a code written in MATLAB (*lsqcurvefit* function).

The experimental data suggested that the path based on di-methoxide (DM) specie is not significant. The kinetic constant of the rate-limiting step of this path ( $k_6$ ) was very low and the quality of the fitting was the same when this path was considered in the kinetic expression and when it was neglected (i.e.,  $k_6 = 0$ ). In addition, a kinetic expression based on this path alone (i.e.,  $k_4 = 0$ ) produce no fitting.

The second term of the denominator of Eq. (11), corresponding to the adsorption of molecular methanol  $K_1 P_M$ , was also found not significant. This suggests the fraction of adsorbed molecular methanol is low in comparison with the other adsorbed species. The fourth term of the denominator of eq. (11) was also eliminated, because it is associated to the di-methoxide (DM) path.

Considering these findings, the expressions of the formation rates of DMC and DMM are simplified to the following equations:

$$r_{DMC} = \frac{k_4 K_1 K_2 K_{O_2} P_M P_{O_2}^{1/2} P_{CO}}{1 + K_1 K_2 K_{O_2} P_M P_{O_2}^{1/2} + K_{CO} P_{CO}} \quad (15)$$

$$r_{DMM} = \frac{k_7 K_1 K_2 K_{O_2}^2 P_M P_{O_2}}{(1 + K_{O_2} P_{O_2}^{1/2}) [1 + K_1 K_2 K_{O_2} P_M P_{O_2}^{1/2} + K_{CO} P_{CO}]} \quad (16)$$

The parameters of Eqs. (15) and (16) were fitted to the experimental data, as shown in Table 3. The model predictions were depicted as lines in Fig. 5, allowing the direct comparison with the experimental data. There are some minor discrepancies between the experiments and the

**Table 3**

Fitted parameters of the kinetic model at 120 °C (SSE = sum of squared errors).

Parameter	Value
$k_4$	0.00729 mol kg <sup>-1</sup> h <sup>-1</sup> kPa <sup>-1</sup>
$k_7$	0.274 mol kg <sup>-1</sup> h <sup>-1</sup>
$K_1K_2$	0.080 kPa <sup>-1</sup>
$K_{O_2}$	0.49 kPa <sup>-1/2</sup>
$K_{CO}$	0.023 kPa <sup>-1</sup>

model predictions at the lowest oxygen concentration for DMM formation rate and the highest oxygen concentration for DMC formation rate (Fig. 5b). Overall, it can be said that the model is able of predicting the formation rates of DMC and DMM within a broad range of reactant concentrations. This is remarked given the complexity of the reaction mechanism and derived model.

The quality of the fitting can also be assessed using the sum of squared errors (SSE), calculated separately for DMC (SSE = 0.0022) and DMM (SSE = 0.0010) data (total SSE = 0.0032). It is evident from the parity plot of Fig. 7 that the model is able of predicting the experimental data with an accuracy of  $\pm 15\%$ .

The significance of the adsorption terms of the kinetic expressions were also checked using the fitted parameters and the range of partial pressures used in the experiments. The range of the different terms of the denominator of Eq. (15) are 1 to 3 for MM adsorption term and 0.4 to 2 for CO adsorption term. In Eq. (16), the oxygen adsorption term is in the range 0.9 to 2. Consequently, neither of these terms can be simplified without affecting the quality of the fitting. Hence, they are considered significative to the model.

#### 4. Conclusions

This study concludes that Cu/Y zeolites, prepared via solid-state ion exchange, can successfully catalyze the oxidative carbonylation of methanol to dimethyl carbonate (DMC). The reaction experiments in a continuous fixed-bed reactor showed an important dependence on temperature of product selectivity. At low temperature (< 140 °C), the main formed compound was the desired DMC product. However, at high temperature (> 180 °C), it was found that DMC decomposed to DME due to the acid centers of the zeolite. Consequently, the optimum recommended operating temperature is 120 °C.

The kinetic experiments, carried out at different concentrations of the reactants, revealed that the formation rate of DMC and DMM were favored by an increase in methanol and oxygen partial pressure, though the dependence was not linear an increase rate levelled at high concentrations. Carbon monoxide only had a marked dependence on DMC formation rate.

A kinetic model for DMC formation rate was derived from the proposed reaction mechanism, based on the formation of adsorbed methoxy species (step in equilibrium) and, then, reaction with carbon monoxide to form monomethyl carbonate (rate-limiting step). Similarly, an expression of DMM formation rate was also derived based on a reaction mechanism with formaldehyde formation as the rate-limiting step. The kinetic and adsorption constants of the model were fitted with good results to the experimental data. The proposed kinetic model constitutes a valuable tool for the scale-up of a process for DMC production, based on the oxidative carbonylation of methanol in the gas phase.

#### CRedit authorship contribution statement

**Mauro Álvarez:** Investigation, Writing – original draft. **Pablo Marín:** Methodology, Supervision, Validation, Writing – review & editing. **Salvador Ordóñez:** Conceptualization, Supervision, Writing – review & editing, Funding acquisition.

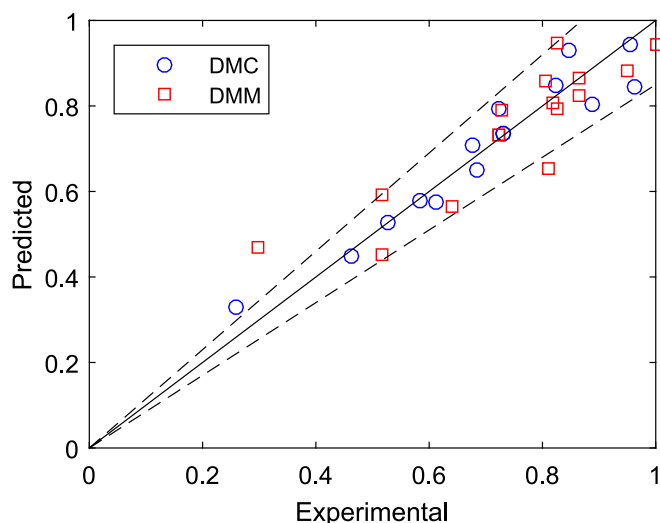


Fig. 7. Parity plot of the model predictions and experimental data (scaled  $\circ$  DMC and  $\square$  DMM formation rates). Dashed lines correspond to  $\pm 15\%$  error limits.

#### Declaration of Competing Interest

The authors declare that they have no known competing financial interests or personal relationships that could have appeared to influence the work reported in this paper.

#### Data availability

Data will be made available on request.

#### Acknowledgements

This work was supported by the Asturian Government (contract GRUPIN AYUD/2021/50450, CRC Research Group).

#### References

- [1] H.-Z. Tan, Z.-Q. Wang, Z.-N. Xu, J. Sun, Y.-P. Xu, Q.-S. Chen, Y. Chen, G.-C. Guo, Review on the synthesis of dimethyl carbonate, *Catal. Today* 316 (2018) 2–12.
- [2] D. Delle Donne, F. Rivetti, U. Romano, Developments in the production and application of dimethyl carbonate, *Appl. Catal. A Gen.* 221 (2001) 241–251.
- [3] Y. Cao, H. Cheng, L. Ma, F. Liu, Z. Liu, Research Progress in the Direct Synthesis of Dimethyl Carbonate from CO<sub>2</sub> and Methanol, *Catal. Surv. Jpn.* 16 (2012).
- [4] X. Gu, X. Zhang, Z. Yang, W. Shen, C. Deng, S. Zeng, X. Zhang, Technical-environmental assessment of CO<sub>2</sub> conversion process to dimethyl carbonate/ethylene glycol, *J. Clean. Prod.* 288 (2021), 125598.
- [5] Y. Ono, Catalysis in the production and reactions of dimethyl carbonate, an environmentally benign building block, *Appl. Catal. A Gen.* 155 (1997) 133–166.
- [6] Y. Zhou, S. Wang, M. Xiao, D. Han, Y. Lu, Y. Meng, Novel Cu–Fe bimetal catalyst for the formation of dimethyl carbonate from carbon dioxide and methanol, *RSC Adv.* 2 (2012) 6831–6837.
- [7] C.B. Kreuzberger, *Chloroformates and Carbonates*, John Wiley & Sons, 2001.
- [8] U. Romano, R. Tesel, M.M. Mauri, P. Rebora, Synthesis of Dimethyl Carbonate from Methanol, Carbon Monoxide, and Oxygen Catalyzed by Copper Compounds, *Industrial & Engineering Chemistry Product Research and Development* 19, 1980, pp. 396–403.
- [9] P. Tundo, M. Selva, The Chemistry of Dimethyl Carbonate, *Acc. Chem. Res.* 35 (2002) 706–716.
- [10] EPA, Air Quality: Revision to Definition of Volatile Organic Compounds-Exclusion of Propylene Carbonate and Dimethyl Carbonate, Environmental Protection Agency, 2009.
- [11] K. Alexandrino, M.U. Alzueta, H.J. Curran, An experimental and modeling study of the ignition of dimethyl carbonate in shock tubes and rapid compression machine, *Combustion and Flame* 188 (2018) 212–226.
- [12] N. Keller, G. Rebmann, V. Keller, Catalysts, mechanisms and industrial processes for the dimethyl carbonate synthesis, *J. Mol. Catal. A Chem.* 317 (2010) 1–18.
- [13] A. Abdalla, D. Liu, Dimethyl carbonate as a promising oxygenated fuel for combustion: a review, *Energies* 11 (2018) 1552.



- [14] M.U. Alzueta, P. Salinas, Á. Millera, R. Bilbao, M. Abián, A study of dimethyl carbonate conversion and its impact to minimize soot and NO emissions, *Proc. Combust. Inst.* 36 (2017) 3985–3993.
- [15] K. Alexandrino, J. Salinas, Á. Millera, R. Bilbao, M.U. Alzueta, Sooting propensity of dimethyl carbonate, soot reactivity and characterization, *Fuel* 183 (2016) 64–72.
- [16] M.A. Pacheco, C.L. Marshall, Review of dimethyl carbonate (DMC) manufacture and its characteristics as a fuel additive, *Energy Fuel* 11 (1997) 2–29.
- [17] F. Viteri, J. Salinas, Á. Millera, R. Bilbao, M.U. Alzueta, Pyrolysis of dimethyl carbonate: PAH formation, *J. Anal. Appl. Pyrolysis* 122 (2016) 524–530.
- [18] P. Kumar, L. Matoh, R. Kaur, U.L. Štangar, Synergic effect of manganese oxide on ceria based catalyst for direct conversion of CO<sub>2</sub> to green fuel additive: catalyst activity and thermodynamics study, *Fuel* 285 (2021), 119083.
- [19] P. Kumar, V.C. Srivastava, U.L. Štangar, B. Mušič, I.M. Mishra, Y. Meng, Recent progress in dimethyl carbonate synthesis using different feedstock and techniques in the presence of heterogeneous catalysts, *Catal. Rev.* (2019) 1–59.
- [20] K. Tomishige, T. Sakaihorii, Y. Ikeda, K. Fujimoto, A novel method of direct synthesis of dimethyl carbonate from methanol and carbon dioxide catalyzed by zirconia, *Catal. Lett.* 58 (1999) 225–229.
- [21] H.-J. Buysch, *Carbonic Esters*, John Wiley & Sons, 2000.
- [22] I.J. Drake, Y. Zhang, D. Briggs, B. Lim, T. Chau, A.T. Bell, The local environment of Cu<sup>+</sup> in Cu–Y zeolite and its relationship to the synthesis of dimethyl carbonate, *J. Phys. Chem. B* 110 (2006) 11654–11664.
- [23] H. Itoh, Y. Watanabe, K. Mori, H. Umino, Synthesis of dimethyl carbonate by vapor phase oxidative carbonylation of methanol, *Green Chem.* 5 (2003) 558–562.
- [24] J. Song, T. Zhao, Y. Du, Supported copper catalysts for direct vapor-phase oxycarbonylation of methanol, *Chin. J. Catal.* 27 (2006) 386–390.
- [25] K. Tomishige, T. Sakaihorii, S.-I. Sakai, K. Fujimoto, Dimethyl carbonate synthesis by oxidative carbonylation on activated carbon supported CuCl<sub>2</sub> catalysts: catalytic properties and structural change, *Appl. Catal. A Gen.* 181 (1999) 95–102.
- [26] M.S. Han, B.G. Lee, I. Suh, H.S. Kim, B.S. Ahn, S.I. Hong, Synthesis of dimethyl carbonate by vapor phase oxidative carbonylation of methanol over Cu-based catalysts, *J. Mol. Catal. A Chem.* 170 (2001) 225–234.
- [27] Y. Zhang, I.J. Drake, D.N. Briggs, A.T. Bell, Synthesis of dimethyl carbonate and dimethoxy methane over Cu-ZSM-5, *J. Catal.* 244 (2006) 219–229.
- [28] S.A. Anderson, T.W. Root, Kinetic studies of carbonylation of methanol to dimethyl carbonate over Cu+X zeolite catalyst, *J. Catal.* 217 (2003) 396–405.
- [29] S.A. Anderson, T.W. Root, Investigation of the effect of carbon monoxide on the oxidative carbonylation of methanol to dimethyl carbonate over Cu+X and Cu+ZSM-5 zeolites, *J. Mol. Catal. A Chem.* 220 (2004) 247–255.
- [30] S.T. King, Reaction Mechanism of Oxidative Carbonylation of Methanol to Dimethyl Carbonate in Cu–Y Zeolite, *J. Catal.* 161 (1996) 530–538.
- [31] J.-K. Nam, M.-J. Choi, D.-H. Cho, J.-K. Suh, S.-B. Kim, The influence of support in the synthesis of dimethyl carbonate by Cu-based catalysts, *J. Mol. Catal. A Chem.* 370 (2013) 7–13.
- [32] Y. Zhang, D.N. Briggs, E. de Smit, A.T. Bell, Effects of zeolite structure and composition on the synthesis of dimethyl carbonate by oxidative carbonylation of methanol on Cu-exchanged Y, ZSM-5, and mordenite, *J. Catal.* 251 (2007) 443–452.
- [33] L. Yan, T. Fu, D. Zhao, J. Wang, N. Narkhede, H. Zheng, G. Zhang, Z. Li, Highly dispersed Cu supported on mesoporous Al-KIT-6 for oxidative carbonylation of methanol to dimethyl carbonate, *Appl. Organomet. Chem.* 34 (2020).
- [34] Z. Li, K. Xie, R.C.T. Slade, High selective catalyst CuCl/MCM-41 for oxidative carbonylation of methanol to dimethyl carbonate, *Appl. Catal. A Gen.* 205 (2001) 85–92.
- [35] Y. Zhang, A.T. Bell, The mechanism of dimethyl carbonate synthesis on Cu-exchanged zeolite Y, *J. Catal.* 255 (2008) 153–161.
- [36] J. Engeldinger, C. Domke, M. Richter, U. Benstrup, Elucidating the role of Cu species in the oxidative carbonylation of methanol to dimethyl carbonate on CuY: an in situ spectroscopic and catalytic study, *Appl. Catal. A Gen.* 382 (2010) 303–311.
- [37] Y. Wang, Z. Liu, C. Tan, H. Sun, Z. Li, High catalytic activity of CuY catalysts prepared by high temperature anhydrous interaction for the oxidative carbonylation of methanol, *RSC Adv.* 10 (2020) 3293–3300.
- [38] C. Perego, S. Peratello, Experimental methods in catalytic kinetics, *Catal. Today* 52 (1999) 133–145.
- [39] J. Perez-Ramirez, R.J. Berger, G. Mul, F. Kapteijn, J.A. Moulijn, The six-flow reactor technology: a review on fast catalyst screening and kinetic studies, *Catal. Today* 60 (2000) 93–109.
- [40] H.S. Fogler, *Elements of Chemical Reaction Engineering*, Pearson, 2008.
- [41] J. Engeldinger, M. Richter, U. Benstrup, Mechanistic investigations on dimethyl carbonate formation by oxidative carbonylation of methanol over a CuY zeolite: an operandoSSITKA/DRIFTS/MS study, *Phys. Chem. Chem. Phys.* 14 (2012) 2183–2191.
- [42] J. Lv, P. Chen, M. Wang, Y. Li, S. Huang, Supplementary mechanism for oxycarbonylation of methanol over CuY catalyst: origin of the oxygen atom in methoxyl and formation of by-products, *Catal. Lett.* 151 (2021) 3334–3342.
- [43] X. Zheng, A.T. Bell, A Theoretical Investigation of Dimethyl Carbonate Synthesis on Cu–Y Zeolite, *J. Phys. Chem. C* 112 (2008) 5043–5047.
- [44] R. Peláez, P. Marín, S. Ordóñez, Effect of formaldehyde precursor and water inhibition in dimethoxymethane synthesis from methanol over acidic ion exchange resins: mechanism and kinetics, *Biofuels Bioprod. Biorefin.* 15 (2021) 1696–1708.